Effects of energy extensivity on the quantum phases of long-range interacting systems

T. Botzung,[1,2,3] D. Hagenmüller ⬤,[1,*] G. Masella,[1] J. Dubail ⬤,[4] N. Defenu,[5] A. Trombettoni,[6] and G. Pupillo[1,†]

[1]*ISIS (UMR 7006) and icFRC, University of Strasbourg and CNRS, 67000 Strasbourg, France*

[2]*Institute for Quantum Information, RWTH Aachen University, D-52056 Aachen, Germany*

[3]*Peter Grünberg Institute, Theoretical Nanoelectronics, Forschungszentrum Jülich, D-52425 Jülich, Germany*

[4]*LPCT (UMR7019), Université de Lorraine and CNRS, F-54506 Vandoeuvre-les-Nancy, France*

[5]*Institute for Theoretical Physics, Heidelberg University, D-69120 Heidelberg, Germany*

[6]*SISSA and INFN, Sezione di Trieste, I-34136 Trieste, Italy*

We investigate the ground state properties of one-dimensional hard-core bosons interacting via a variable long-range potential using the density matrix renormalization group. We show that restoring energy extensivity in the system, which is done by rescaling the interaction potential with a suitable size-dependent factor known as Kac's prescription, has a profound influence on the low-energy properties in the thermodynamic limit. While an insulating phase is found in the absence of Kac's rescaling, the latter leads to a new metallic phase that does not fall into the conventional Luttinger liquid paradigm. We discuss a scheme for the observation of this new phase using cavity-mediated long-range interactions with cold atoms. Our findings raise fundamental questions on how to study the thermodynamics of long-range interacting quantum systems.

I. INTRODUCTION

Long-range (LR) interacting systems are characterized by highly nonlocal couplings typically decaying as a power law for large distances. Famous examples of such systems include self-gravitating clusters [1], ferromagnetic materials [2], non-neutral plasmas [3], cavity-QED systems [4], and one-dimensional quantum wires [5]. Recent progress in the realization of artificial lattices of cold gases with sizable LR interactions has stimulated considerable interest [6–22]. In parallel, theoretical studies of the ground state of LR spin models have revealed anomalous critical exponents [23–25] and decay of correlations [26–31], as well as the existence of new quantum phases [32–37].

An archetypal LR quantum model consists of one-dimensional (1D) fermions interacting via a $1/r$ (unscreened) Coulomb potential, with r the distance separating two particles. Schulz showed using bosonization techniques that the ground state of this model is a peculiar metal resembling a classical Wigner crystal, with very slow decay of the charge correlations associated with the plasmon mode [38,39]. This result was confirmed numerically using density matrix renormalization group (DMRG) [40] and Monte Carlo methods [41–43]. In the presence of a lattice at commensurate fillings, it was shown that while the metallic behavior is surprisingly enhanced as compared to short-range interactions for small system size, the ground state ultimately enters an insulating phase in the thermodynamic limit [44–47].

The *strong* LR regime for a d-dimensional system with volume $\mathcal{V}$ is achieved when the power-law exponent α entering the potential $V(r) \propto 1/r^\alpha$ is such that $0 \leqslant \alpha \leqslant d$. This regime is typically associated with unusual thermodynamic properties such as a nonextensive energy $E \sim \mathcal{V}^{2-\frac{\alpha}{d}}$ leading to an ill-defined thermodynamic limit [48]. Furthermore, the total energy cannot be obtained by summing up the energies of different subsystems as is usually the case for short-range interactions [49,50]. This nonadditivity appears as a fundamental property of LR models and leads to exotic behaviors including the breaking of ergodicity, the existence of slow relaxation processes, and the inequivalence of statistical ensembles [51–55]. In contrast, extensivity can be restored by rescaling the interaction potential with a volume-dependent factor Λ, which is known as the Kac's prescription [56]. The latter is systematically used to study the thermodynamic properties of classical spin models with LR interactions [57–61], where the dynamical properties with and without Kac's prescription are the same provided proper rescaling of timescales [62,63]. However, the latter statement does not hold true with quantum variables, thereby questioning the use of the Kac's prescription in quantum models. It is an interesting question to investigate whether ground state phases can be also modified by Kac's rescaling, which would raise fundamental questions on how to tackle the thermodynamics of long-range interacting quantum models.

Here we study a 1D periodic chain of interacting hard-core bosons in the strong LR regime at half-filling, using the Luttinger liquid (LL) theory combined with DMRG calculations [64] for large system sizes ($\gtrsim$200 sites). We consider the general model with $0 \leqslant \alpha \leqslant 1$, which interpolates between the infinite-range case ($\alpha = 0$) and Coulomb repulsion ($\alpha = 1$) studied in Ref. [45]. In the absence of Kac's rescaling we find
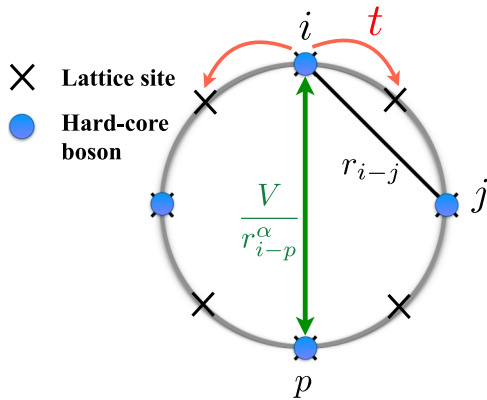
*dhagenmuller@unistra.fr

†pupillo@unistra.fr

FIG. 1. Sketch of the physical system described by the Hamiltonian Eq. (1), which consists of a circular chain with periodic boundary conditions.

FIG. 2. Finite-size scaling of the single-particle gap Δ computed with DMRG at half-filling $\langle n_i \rangle = 0.5$, for $\alpha = 1$ and different interaction strengths V (in units of the hopping energy t). While an insulating phase ($\Delta \neq 0$) is found without Kac's rescaling (a) and (b), the latter leads to a metallic phase ($\Delta = 0$) in the thermodynamic limit (c) and (d). Extrapolation for $L \to \infty$ is obtained by fitting the numerical data with $\Delta(L) = b + \frac{c}{L} + \frac{d}{L^2}$ (dotted lines). The finite-size scaling of the ground state energy per particle is shown in (b) and (d). The error bars are too small to be visible (see Appendix B).

that the ground state consists of an insulating gapped phase in the thermodynamic limit, extending the results of Ref. [45] to the whole range $0 < \alpha \leqslant 1$. In stark contrast we demonstrate that Kac's rescaling leads to a metallic phase for any finite strength of the interaction, which is found to be incompatible with a standard LL. This unconventional behavior can be traced back to a mean-field term in the Hamiltonian, exact for $\alpha = 0$, which leads to qualitatively different behaviors for the charge gap and the correlation functions. Restoring extensivity is further shown to eliminate the plasmon modes while preserving the LR character of the potential, and with it some inherent properties of the strong LR regime such as nonadditivity.

The remainder of the paper is organized as follows. In Sec. II we introduce the model under consideration. In Sec. III we discuss the different phases of the model (metallic vs insulating) depending on whether Kac's rescaling of the interaction potential is used or not. These results are obtained from numerical calculations of the charge gap (Sec. III A), the Luttinger parameters (Sec. III C), and from the low-energy properties of the model (Sec. III B). In Sec. IV we demonstrate that the metallic phase found in the presence of Kac's rescaling is incompatible with a standard LL. We provide a conclusion in Sec. V.

II. MODEL

We consider the following Hamiltonian:

$$H = -t \sum_{i=1}^{L} (a_i^\dagger a_{i+1} + \text{H.c.}) + \sum_{i>j} V_{i-j}^{(\alpha)} n_i n_j, \quad (1)$$

where the operator a_i ($a_i^\dagger$) annihilates (creates) a hard-core boson on site $i = 1, \ldots, L$, and $n_i = a_i^\dagger a_i$ is the local density. The interaction potential reads

$$V_{i-j}^{(\alpha)} = \frac{V}{\Lambda_\alpha(L) r_{i-j}^\alpha}, \quad V > 0,$$

where $r_{i-j} = (La/\pi) \sin(\pi|i-j|/L)$ for $L \gg 1$ as we assume periodic boundary conditions (Fig. 1). The nearest-neighbor hopping t and lattice spacing a are set to $t \equiv a \equiv 1$,
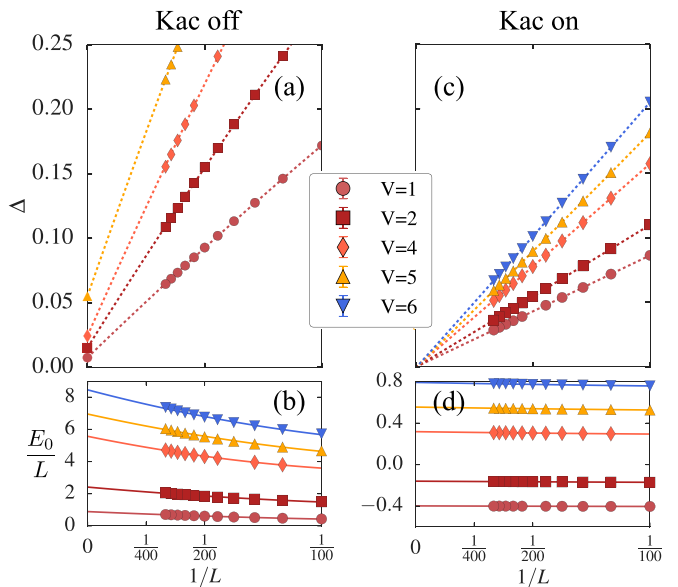
and we use DMRG to compute the different observables. The detailed numerical methods are provided in Appendix B.

Kac's rescaling of the interaction potential is included via the function $\Lambda_\alpha(L) = 1$ for $\alpha > 1$ (absence of Kac's rescaling), $\Lambda_\alpha(L) = \log(L)$ in the marginal case $\alpha = 1$, and $\Lambda_\alpha(L) = L^{1-\alpha}$ in the strong LR regime $\alpha < 1$. Note that the XXZ Heisenberg model with LR coupling along the z direction and short-range coupling along x and y can be mapped either onto hard-core bosons Eq. (1) or spinless fermions via a Jordan-Wigner transformation. In Appendix A we discuss a realization of this model in the infinite-range case $\alpha = 0$ using cavity-mediated interactions between cold atoms. Due to the normalization of the electromagnetic energy, this interaction scales as $\sim 1/L$ and thus automatically includes a Kac's rescaling. The range $0 < \alpha < 3$ can in principle be realized with trapped ions [11] where V, α, and L can be tuned independently, thus allowing us to compare the situations with and without Kac's rescaling.

III. METALLIC VERSUS INSULATING PHASE

A. Charge gap

The main result of our work is summarized in Fig. 2, where we compute the single-particle charge gap

$$\Delta = E_0(N+1) + E_0(N-1) - 2E_0(N)$$

for $\alpha = 1$ and different interaction strengths V. Here $E_0(N)$ denotes the energy of the ground state with N particles. The situation without Kac's rescaling [$\Lambda_1(L) = 1$, Figs. 2(a) and 2(b)] has been already investigated in Ref. [45], and features a

nonextensive energy. In this case we find that the gap $\Delta(L \gg 1) \neq 0$ for any $V > 0$, which indicates an insulating phase in the thermodynamic limit consistently with the conclusion of Ref. [45]. These results are drastically modified when using the Kac's prescription. By rescaling the interaction potential [$\Lambda_1(L) = \log(L)$, Fig. 2(c) and 2(d)], we find that while extensivity is clearly restored, $\Delta \sim 1/L$ for all $V > 0$. This result indicates a metallic behavior in the thermodynamic limit observed in the whole range $0 \leqslant \alpha \leqslant 1$ (not shown).

B. Low-energy properties

In order to understand the physical origin of the significant difference between the extensive and nonextensive models, we investigate the low-energy properties of Eq. (1) using the LL theory. A convenient bosonic representation of H in terms of the continuous variable $x \equiv ja$ can be obtained by treating the interaction potential as a perturbation [5]

$$H = \frac{1}{2\pi} \int dx \left(uK(\pi \Pi)^2 + \frac{u}{K} \nabla^2 \phi - \frac{g}{\pi a^2} \cos(4\phi) \right), \quad (2)$$

where $\Pi(x)$ and $\phi(x)$ and are canonically conjugate bosonic fields depending on the long wavelength fluctuations of the fermion density. The so-called Luttinger parameters u and K are related by [45] (see Appendix C)

$$uK = v_{\text{F}},$$

$$\frac{u}{K} = v_{\text{F}} + \frac{1}{\pi} \sum_{r=1}^{L} V_r^{(\alpha)}[1 - \cos(2k_{\text{F}}r)], \quad (3)$$

with v_{F} and k_{F} the Fermi velocity and Fermi wave vector, respectively. The first two (quadratic) terms of Eq. (2) describe how the properties of the noninteracting LL are renormalized by the interactions. In particular, K determines the decay of the single-particle correlation function

$$\langle a_i^\dagger a_j \rangle \sim r_{i-j}^{-1/(2K)}.$$

The third term in Eq. (2) stems from scattering processes across the Fermi surface where the particle momentum is conserved up to a reciprocal lattice vector. It is usually denoted as umklapp term and scales with the strength

$$g \equiv \sum_{r=1}^{L} V_r^{(\alpha)} \cos(2k_{\text{F}}r). \quad (4)$$

For a finite g it is possible to show using a renormalization-group study [5] of the Hamiltonian Eq. (2) for $\alpha > 1$ that the system goes from an insulating to a metallic phase as K is increased above a critical value K_c [65]. At half-filling and neglecting multiple umklapp scattering [66], the critical value is $K_c = 0.5$. Note that in the case of a nearest-neighbor interaction $\alpha \to \infty$, such a metal-insulator transition occurs at $V = 2t$ [67].

We consider a half-filled band $\langle n_i \rangle = 0.5$, which provides $k_{\text{F}} = \pi/2$ and $v_{\text{F}} = 2$. In the absence of Kac's rescaling the first sum $\sum_r V_r^{(\alpha)}$ entering Eq. (3) diverges in the thermodynamic limit $\sim \log(L)$ for $\alpha = 1$ and $\sim L^{1-\alpha}/(1-\alpha)$ for $0 \leqslant \alpha < 1$. The second sum $\sum_r V_r^{(\alpha)} \cos(2k_{\text{F}}r)$ entering Eqs. (3) and (4) is bounded due to the alternating sign. Therefore, while the umklapp scattering strength g remains finite, the
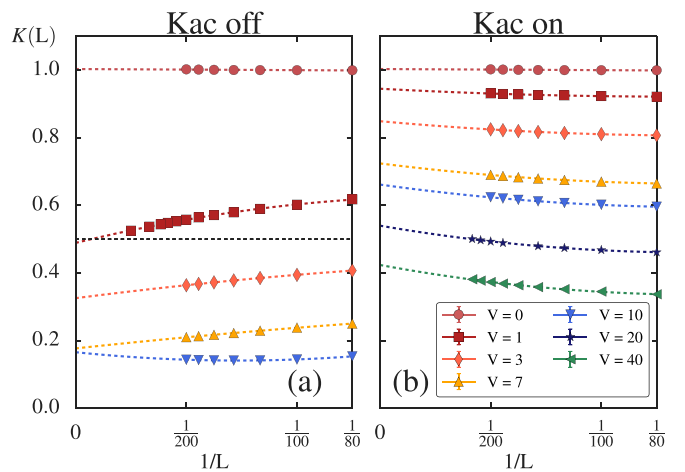

FIG. 3. Luttinger parameter K computed numerically at half-filling for $\alpha = 0.5$ and different V, by fitting the correlation function $\langle a_i^\dagger a_j \rangle$ [70]. The critical value $K_c = 0.5$ indicating the metal-insulator transition with nearest-neighbor interaction is displayed as a black dashed line. In the absence of Kac's rescaling (a), K decreases when increasing L, lying below the critical line for $L \to \infty$ (insulating phase). In contrast, K increases with L in the presence of Kac's rescaling (b), and remains finite even for very large V (metallic phase). Extrapolation in the thermodynamic limit is obtained by fitting the data with the same function as in Fig. 2 (dotted lines). The error bars are too small to be visible (see Appendix B).

Luttinger parameter $K \to 0$ for $0 < \alpha \leqslant 1$ and $V > 0$ in the thermodynamic limit consistently with an insulating phase.

We find that rescaling the interaction potential with the factor $\Lambda_\alpha(L) = \log(L)$ for $\alpha = 1$ and $\Lambda_\alpha(L) = L^{1-\alpha}$ for $\alpha < 1$ strongly affects the competition between K and g. In this case the long-wavelength divergence is removed since $\lim_{L\to\infty} \sum_r V_r^{(\alpha)} = V$ for $\alpha = 1$ and $\lim_{L\to\infty} \sum_r V_r^{(\alpha)} = V/(1-\alpha)$ for $\alpha < 1$. This suggests a metallic phase for $0 < \alpha \leqslant 1$, since K remains finite and $g \to 0$ for any finite $V > 0$ in the thermodynamic limit as seen from Eqs. (3) and (4).

The above arguments cannot be used in the infinite-range case $\alpha = 0$ since the series $\sum_r V_r^{(\alpha)} \cos(2k_{\text{F}}r)$ does not have a unique limit for $L \to \infty$. Nevertheless, this particular case can be solved exactly and corresponds to a metallic (free fermions) phase with charge correlations $\langle a_i^\dagger a_j \rangle \sim r_{ij}^{-1/2}$, regardless of the presence or absence of Kac's rescaling [68] (see Appendix D).

C. Luttinger parameters

In order to gain further insights we first compute the Luttinger parameter K by fitting the correlation function $\langle a_i^\dagger a_j \rangle$. This parameter is shown in Fig. 3 for $\alpha = 0.5$ and different V. We observe two opposite trends depending on whether Kac's rescaling is present or not. In the latter case [Fig. 3(a)] K decreases when increasing L and lies below the critical value $K_c = 0.5$ for $L \to \infty$, which indicates an insulating phase. The case with Kac's rescaling is shown in Fig. 3(b), where a finite K is found for all V in the thermodynamic limit.
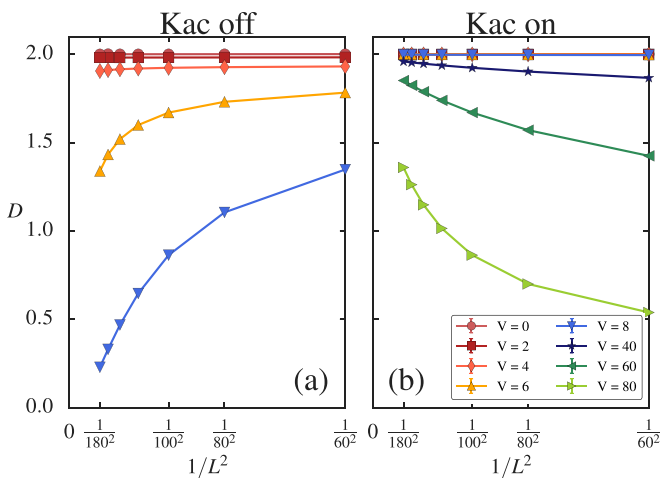
3

FIG. 4. Charge stiffness D computed numerically from Eq. (5) at half-filling, as a function of $1/L^2$ for $\alpha = 0.5$ and different V. The magnetic flux Φ is implemented via the twisted boundary condition $a_1 = e^{i\Phi}a_{L+1}$ [66]. Two opposite trends are observed depending on whether Kac's rescaling is present (b) or not (a). While $D \to 0$ for $L \to \infty$ in the latter case (insulator), D remains finite in the former case (metal). The error bars are too small to be visible (see Appendix B).

We then compute the charge stiffness [5]

$$D = \pi L \left| \frac{\partial^2 E_0(\Phi)}{\partial \Phi^2} \right|_{\Phi=0}, \quad (5)$$

which is proportional to the Drude weight [69] and therefore provides valuable information on the metallic or insulating properties of the system. Moreover, it also gives a direct measure of the umklapp scattering strength. A large D corresponds to a good metal, while an insulating phase features $D = 0$. The charge stiffness is computed numerically from the ground state energy E_0 by threading a flux Φ through the circular chain, and shown in Fig. 4 as a function of $1/L^2$ for $\alpha = 0.5$. In the absence of Kac's rescaling [Fig. 4(a)] D decreases when increasing L for any finite V. The latter drives the system towards an insulating phase ($D \to 0$) in the thermodynamic limit. In contrast, D increases with L in the presence of Kac's rescaling [Fig. 4(b)], which confirms the metallic behavior. In the thermodynamic limit we find that $D \approx v_F$ even for very large V, in surprisingly good agreement with the LL prediction $D = uK$ and Eq. (3). Note that we have performed a full numerical study showing that the conclusions drawn from Figs. 3 and 4 can be unambiguously extended to the whole range $0 \leqslant \alpha \leqslant 1$.

IV. BREAKDOWN OF LL THEORY

Now that we have demonstrated the metallic character of the ground state, we check the validity of the LL theory in Fig. 5 by computing the parameter K for $L \to \infty$ and $\alpha = 0.5$ in three different ways: From the single-particle correlation function $\langle a_i^\dagger a_j \rangle$ (see above); from the static structure factor

$$S(q) = \frac{1}{L} \sum_{i,j} e^{iq|i-j|} (\langle n_i n_j \rangle - \langle n_i \rangle \langle n_j \rangle) \quad (6)$$
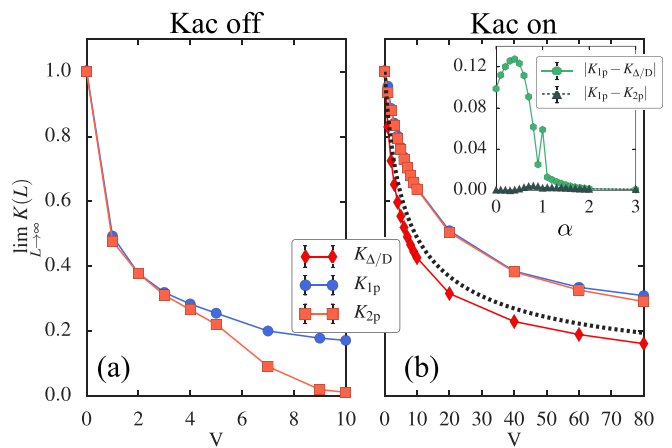

FIG. 5. Luttinger parameter K extrapolated for $L \to \infty$ versus V at half-filling and for $\alpha = 0.5$, without (a) and with (b) Kac's rescaling. K is computed in three different ways: From the single-particle correlations (K_{1p}), the structure factor (K_{2p}), and from the gap and the charge stiffness ($K_{\Delta/D}$). The formula obtained from Eq. (3) is displayed as a dotted line. Inset: $|K_{1p} - K_{2p}|$ and $|K_{1p} - K_{\Delta/D}|$ versus α for $V = 1.5$. A discrepancy between K_{1p} and K_{2p} is observed without Kac's rescaling, which indicates the breakdown of the LL theory (insulator). In contrast, the property $K_{1p} = K_{2p}$ observed with Kac's rescaling even for large V suggests a metallic phase, which is not captured by the conventional LL theory. The error bars are too small to be visible (see Appendix B).

as $K = LS(q = \frac{2\pi}{L})$; and from the relations

$$\pi \frac{u}{K} = \frac{\partial \Delta}{\partial (1/L)}$$

and $uK = D$ stemming from the LL theory [5]. In the absence of Kac's rescaling [Fig. 5(a)] a discrepancy between the values of K extracted from the two correlation functions (labeled K_{1p} and K_{2p} in the figure) is observed, which indicates the breakdown of the LL theory related to the opening of a gap (insulating phase). The agreement obtained for small V is attributed to the metal-like character at finite L consistently with the data shown in Fig. 3. In the presence of Kac's rescaling [Fig. 5(b)] K_{1p} and K_{2p} match well up to very large V, while they match neither the formula

$$K = \frac{1}{\sqrt{1 + V/[\pi v_F(1-\alpha)]}}$$

(dotted line) stemming from Eq. (3) nor K obtained from Δ and D (labeled $K_{\Delta/D}$ in the figure). We find that this discrepancy holds in the entire range $0 \leqslant \alpha \leqslant 1$ (see inset), implying a breakdown of LL theory in the strong LR regime. For $\alpha > 0$ this breakdown is only partial since numerics indicate that both $K_{\Delta/D}$ and $K_{1p,2p}$ maintain the functional form

$$K = \frac{1}{\sqrt{1 + \gamma V/(\pi v_F)}}, \quad (7)$$

with γ finite for all V [see Fig. 5(b)]. This is, however, not true for the mean-field case $\alpha = 0$ which can be solved exactly (see Appendix D). In this case, the mean-field Hamiltonian contains a term $\propto N^2$ in addition to a free-fermion part. Since the Hamiltonian conserves the number of particles, the term

4

$\propto N^2$ is a simple offset and the free-fermion result $K_{1p,2p} = 1$ is thus obtained from equal-time correlation functions for all V. In contrast for $K_{\Delta/D}$ we obtain Eq. (7) with $\gamma = 1$. This is due to the fact that the charge gap is constructed from the ground state energy in different charge sectors, and therefore the term $\propto N^2$ leads to

$$\Delta \sim \frac{V + 2\pi t}{L}$$

for $L \to \infty$. This term makes the excitation spectrum of the Hamiltonian incompatible with that of a standard LL (see Appendix D). In the short-range case $\alpha \gg 1$ all methods predict the same K as expected from the LL theory (see inset). The demonstration of this gapless, critical metallic phase that is neither fully described by the LL theory nor the mean-field approach for $0 < \alpha \leqslant 1$ is a central result of this work. While here we focused on the case of half-filling, this phase appears in fact for all densities.

In Appendix C we show that the long-wavelength excitations of this phase have a linear dispersion, similar to a LL with purely short-range interactions (as normal He-3 for instance). This can be readily shown by considering the continuous Hamiltonian Eq. (2) with interaction potential $V^{(\alpha)}(x) = V/(x^2 + a^2)^{\alpha/2}$. The diagonalization of this Hamiltonian in Fourier space provides the plasmon dispersion relation

$$\omega(q) = v_{\mathrm{F}} q \sqrt{1 + \frac{V^{(\alpha)}(q)}{\pi v_{\mathrm{F}}}}.$$

Kac's rescaling eliminates the long-wavelength divergence of the Fourier component $V^{(\alpha)}(q \to 0)$ and therefore leads to the dispersion relation of a metal with short-range interactions $\omega(q) \sim v_{\mathrm{F}} q$. Note that since the algebraic character of the interaction potential is preserved when using the Kac's prescription, the latter is thus "weaker" than Thomas-Fermi screening which turns the LR interaction into a short-range one.

V. CONCLUSION

In conclusion, we have shown that the low-energy properties of 1D hard-core bosons interacting via a LR potential are fundamentally modified in the strong LR regime when applying the Kac's prescription, which restores energy extensivity and a well-defined thermodynamic limit [71]. We find that the linear excitation spectrum of our unconventional, extensive metallic phase is also present for $d > 1$ in the case of Coulomb repulsion ($\alpha = 1$). It would be therefore an interesting perspective to investigate the properties of this phase in higher dimensions using, e.g., Monte Carlo techniques [34,72]. This is particularly relevant since two-dimensional lattices with cavity-mediated long-range interactions can also be realized with cold atoms [73]. It is another exciting prospect to study the exotic statistical and thermodynamical properties of our unconventional quantum liquid that are expected to occur in analogy with classical [49–54] and semi-classical [55] models.
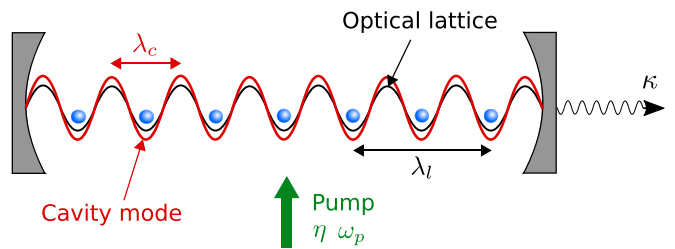

FIG. 6. N two-level atoms (blue spheres) trapped in a 1D optical lattice (black) with depth V_l and wavelength λ_l. The atoms strongly interact with a cavity mode (red) of wavelength $\lambda_c = \lambda_l/2$ and decay rate κ, and are coherently driven by a transverse pump with frequency ω_p and strength η.

APPENDIX A: EXTENSIVE CAVITY-MEDIATED LONG-RANGE INTERACTIONS

In the following Appendixes we discuss a possible implementation of our 1D hard-core boson Hamiltonian with infinite-range interactions using cavity-mediated interactions between cold atoms (Appendix A). We provide details about the numerical methods including an error analysis (Appendix B), and show that the plasmon mode of a d-dimensional system of long-range (LR) interacting fermions is suppressed when using the Kac prescription in the strong long-range regime $\alpha \leqslant d$ (Appendix C). We solve the infinite-range case $\alpha = 0$ exactly, showing that the system is in a metallic (free fermion) phase with a charge gap $\Delta \sim (V + 2\pi t)/L \to 0$ for $L \to \infty$, which is incompatible with the Luttinger liquid theory (Appendix D).

We propose a possible implementation of our 1D hard-core boson Hamiltonian Eq. (1) with infinite-range interactions ($\alpha = 0$) using an atomic quantum gas trapped in an optical lattice and embedded in a cavity. The physical system is shown in Fig. 6: N two-level bosonic atoms with mass m forming a Bose-Einstein condensate are loaded into a 1D optical lattice of depth V_l and period $\lambda_l/2$ along the x direction. The atoms with transition frequency ω_a strongly interact with a cavity mode of frequency ω_c and period $\lambda_c = \lambda_l/2$, and are coherently driven (transversally) by a laser field with frequency ω_p and strength η. The lattice and cavity wave vectors are $k_l = 2\pi/\lambda_l$ and $k_c = 2\pi/\lambda_c$, respectively.

In the frame rotating with the laser frequency, the Hamiltonian (in frequency units) for a single atom in the rotating-wave approximation reads [73,74]

$$H = H_0 - \Delta_c c^\dagger c - \frac{\Delta_a}{2}\sigma_z + g\cos(k_c x)(\sigma_+ c + c^\dagger \sigma_-)$$
$$+ \eta(\sigma_- + \sigma_+), \qquad (A1)$$

with $\Delta_c = \omega_p - \omega_c$, $\Delta_a = \omega_p - \omega_a$, and

$$H_0 = -\frac{\hbar}{2m}\frac{\partial^2}{\partial x^2} + V_l\cos^2(k_l x)$$

the optical lattice Hamiltonian. The cavity mode annihilation operator is denoted as c and the atom with ground state $|g\rangle$ and excited state $|e\rangle$ is described by the Pauli matrices $\sigma_- = |g\rangle\langle e|$ ($\sigma_+ = \sigma_-^\dagger$) and $\sigma_z = |e\rangle\langle e| - |g\rangle\langle g|$. We are interested in the dispersive regime where the atom-pump detuning Δ_a is much larger than the atom-cavity coupling strength g, i.e., $g/\Delta_a \ll 1$. In this case, spontaneous emission is negligible and the atom excited state can be adiabatically eliminated [74]. Replacing σ_z by $\langle g|\sigma_z|g\rangle = -1$ in the equation of motion $\frac{d\sigma_-}{dt} = -i[\sigma_-, H]$, the steady-state solution $\frac{d\sigma_-}{dt} = 0$ is

$$\sigma_- = \frac{2\eta}{\Delta_a} + \frac{2g}{\Delta_a}\cos(k_c x)c.$$

Using this solution in Eq. (A1) leads to the Hamiltonian (up to constant terms)

$$H = H_0 - \Delta_c c^\dagger c + \eta_{\text{eff}}\cos(k_c x)(c + c^\dagger) + U_0\cos^2(k_c x)c^\dagger c, \qquad (A2)$$

where $U_0 = 4g^2/\Delta_A$, and where $\eta_{\text{eff}} = 4g\eta/\Delta_a$ represents an effective pump through atomic scattering into the cavity mode. Now turning to the many-atom system, it is convenient to expand the atom field operators $\Psi(x)$ in the basis of Wannier functions $\phi(x - x_j)$ localized on the lattice sites x_j ($j = 1, 2, \ldots, L$), which are obtained from the Bloch eigenstates of H_0. The second-quantized Hamiltonian takes the form

$$H_{\text{sq}} = \int dx\,\Psi^\dagger(x)H\Psi(x)$$
$$+ \frac{1}{2}\frac{4\pi a_s\hbar}{m}\int dx\,\Psi^\dagger(x)\Psi^\dagger(x)\Psi(x)\Psi(x), \qquad (A3)$$

where the second term is the contact interaction induced by s-wave scattering with characteristic length a_s. Using $\Psi(x) = \sum_j a_j\phi(x - x_j)$ with a_j the annihilation operator of an atom at site x_j, the many-body Hamiltonian reads [74]

$$H_{\text{sq}} = -\sum_{i,j} t_{ij}a_i^\dagger a_j - \Delta_c c^\dagger c + \eta_{\text{eff}}\sum_{i,j} J_{ij}a_i^\dagger a_j(c^\dagger + c)$$
$$+ U_0\sum_{i,j}\widetilde{J}_{ij}a_i^\dagger a_j c^\dagger c + \frac{U}{2}\sum_i a_i^\dagger a_i(a_i^\dagger a_i - 1). \quad (A4)$$

The contact interaction strength reads $U = \frac{4\pi a_s\hbar}{m}\int dx\,|\phi(x)|^4$, and the overlap integrals

$$t_{ij} = -\int dx\,\phi^*(x - x_i)H_0\phi(x - x_j), \qquad (A5)$$

$$J_{ij} = \int dx\,\phi^*(x - x_i)\cos(k_c x)\phi(x - x_j), \qquad (A6)$$

$$\widetilde{J}_{ij} = \int dx\,\phi^*(x - x_i)\cos^2(k_c x)\phi(x - x_j). \qquad (A7)$$

When the overlap between the Wannier functions localized on two different sites is sufficiently small, one can keep only the nearest-neighbor contribution $x_i = x_j \pm \lambda_l/2$ in Eq. (A5). Note that the on-site contribution $x_i = x_j$ simply provides an energy offset and can thus be discarded. On the other hand, the particular choice $\lambda_c = \lambda_l/2$ implies that $\cos(k_c x_i) = -1$ for all i, in contrast to Ref. [73] where the condition $\lambda_c = \lambda_l$ leads to an alternating sign between even and odd sites. Keeping only the on-site contribution $x_i = x_j$ in Eqs. (A6) and (A7), and further assuming normalized Wannier functions $\int dx|\phi(x)|^2 = 1$ the Hamiltonian Eq. (A4) takes the form

$$H_{\text{sq}} = -t\sum_i(a_i^\dagger a_{i+1} + \text{H.c.}) - \Delta_c c^\dagger c - \eta_{\text{eff}}\hat{N}(c^\dagger + c)$$
$$+ U_0\hat{N}c^\dagger c + \frac{U}{2}\sum_i n_i(n_i - 1), \qquad (A8)$$

where $\hat{N} = \sum_i n_i = \sum_i a_i^\dagger a_i$ and

$$t = -\int dx\,\phi^*(x)\left[-\frac{\hbar}{2m}\frac{\partial^2}{\partial x^2} + V_l\cos^2(k_l x)\right]\phi\left(x \pm \frac{\lambda}{2}\right).$$

We now proceed with the adiabatic elimination of the cavity mode [74] under the assumption that $|\Delta_c + i\kappa| \gg \Delta_a, g$. We use $\frac{dc}{dt} = -i[c, H_{\text{sq}}] - \kappa c$, which can be easily derived from the equation of motion $\frac{d\rho}{dt} = -i[H_{\text{sq}}, \rho] + \mathcal{L}\rho$ of the density operator ρ with the dissipative contribution

$$\mathcal{L}\rho = \kappa(2c\rho c^\dagger - c^\dagger c\rho - \rho c^\dagger c).$$

The steady-state solution $\frac{dc}{dt} = 0$ reads

$$c = -\frac{\eta_{\text{eff}}\hat{N}}{(\Delta_c + i\kappa)\left(1 - \frac{U_0}{\Delta_c + i\kappa}\hat{N}\right)}, \qquad (A9)$$

which we expand up to first order in the small parameter $\frac{U_0}{\Delta_c + i\kappa}$. Using this expansion in Eq. (A8), we obtain the Hamiltonian

$$H = -t\sum_{i=1}^L(a_i^\dagger a_{i+1} + \text{H.c.}) + \frac{U}{2}\sum_{i=1}^L n_i(n_i - 1)$$
$$+ W\sum_{i>j} n_i n_j, \qquad (A10)$$

where

$$W = \frac{2\Delta_c\eta_{\text{eff}}^2}{\Delta_c^2 + \kappa^2} = 32\Delta_c\left(\frac{g}{\Delta_a}\right)^2\frac{\eta^2}{\Delta_c^2 + \kappa^2}.$$

Since the second term $\propto U \gg W$ in Eq. (A10) provides the hard-core boson constraint, this Hamiltonian is identical to Eq. (1) with the identification $V_{i-j}^{(0)} = \frac{V}{\Lambda_0(L)} \equiv W$ (infinite-range interaction $\alpha = 0$). Importantly energy extensivity [$\Lambda_0(L) = L$] is here ensured by the g^2 factor in W since the atom-cavity coupling strength g depends on the cavity mode volume due to the normalization of the electromagnetic energy [75], namely $g \sim 1/\sqrt{L}$. The parameters t and W of the Hamiltonian Eq. (A10) can be tuned by changing, e.g., the optical lattice depth V_l and the cavity-pump detuning Δ_c, respectively.
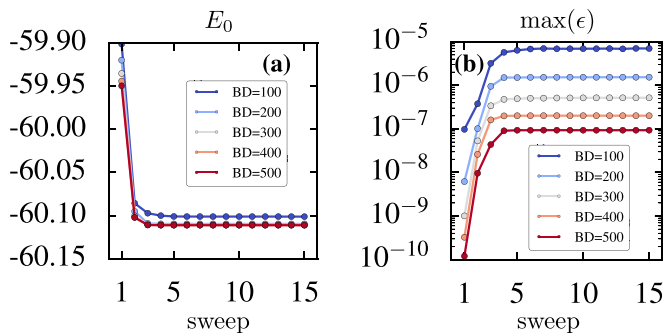
FIG. 7. (a) Ground state energy E_0 versus number of sweeps for different BD. (b) Maximum truncation error ϵ during each sweep for different BD. Parameters are $\langle n_i \rangle = 0.5$ (half-filling), $\alpha = 0.5$, $L = 200$, and $V = 1$.

APPENDIX B: NUMERICAL METHODS

DMRG is a variational method minimizing the energy over quantum states described by matrix product states, i.e., products of matrices. The dimension of these matrices is an indicator of the Hilbert space truncation and is referred to as "bond dimension" (BD) in the following. Note that DMRG provides exact results in the limit of an infinite BD. For a finite BD, the precision of the results is determined by the convergence with the BD and the number of optimization cycles (called sweeps) over the lattice, as well as the truncation error ϵ (sum of discarded squared singular values) during each optimization process.

We first look at the convergence of the ground state energy with the number of sweeps [Fig. 7(a)], and check that the truncation error remains small for a large enough BD [Fig. 7(b)]. Note that the maximum truncation error $\max(\epsilon) < 10^{-7}$ for the BD considered in this work (BD = 500). In order to extract the error on the energy we compute $|E_0(\text{BD} = \infty) - E_0(\text{BD} = 512)| \approx 10^{-5}$. $E_0(\text{BD} \to \infty)$ is obtained by extrapolating the ground state energy in the limit of infinite bond

dimension. Now that we have computed E_0 the uncertainty on the compressibility, the charge stiffness, and the Luttinger parameter $K_{\Delta/D}$ can be obtained as follows. The single-particle gap Δ is shown in Fig. 8(a) as a function of the inverse system size $1/L$ (error bars $\sim 10^{-4}$ are not visible). The best fits of the form $\Delta(L) = b + \frac{c}{L}$ are displayed by continuous lines. Importantly we note that the (small) standard error on E_0 (or equivalently on Δ) are included in our fitting procedure. The compressibility

$$y \equiv \frac{u}{K} = \frac{\delta\Delta}{\pi\delta(1/L)}$$

is directly extracted from the fit, and the uncertainty in the fit parameters is obtained from the least-square method. The uncertainty in the compressibility Δ_y obtained by following this procedure is shown in Fig. 8(b) as a function of V. This error increases with V due to important size effects. Indeed in the limit $V \to \infty$ for a fixed L, the system evolves towards a classical insulating state that DMRG fails to describe. However, we show in the following that the relative error on $K_{\Delta/D}$ plotted in Fig. 5 remains small enough for all V considered in this work.

The charge stiffness is obtained from the formula

$$D = \pi L \left| \frac{\partial^2 E_0(\Phi)}{\partial \Phi^2} \right|_{\Phi=0}$$

[see Eq. (5)] with a flux interval $\delta\Phi = 2\pi \times 0.02$. In Fig. 8(c) we show an example of the ground state energy as a function of Φ for $V = 1$ and $L = 200$. The red line is the best fit of the form $E_0(\Phi) = a + b\Phi + \frac{c}{2}\Phi^2$, with standard error obtained from the least-square method. The charge stiffness can be directly inferred from the parameter c as $D = c\pi L$, and extrapolations of D in the thermodynamic limit $L \to \infty$ for different V are shown in Fig. 8(d). Here the error bars originating from the fit in Fig. 8(c) are smaller than the symbols and thus not visible. The dotted lines are fits of the form $D(L) = b + \frac{c}{L} + \frac{d}{L^2}$, with standard error in the fit parameters
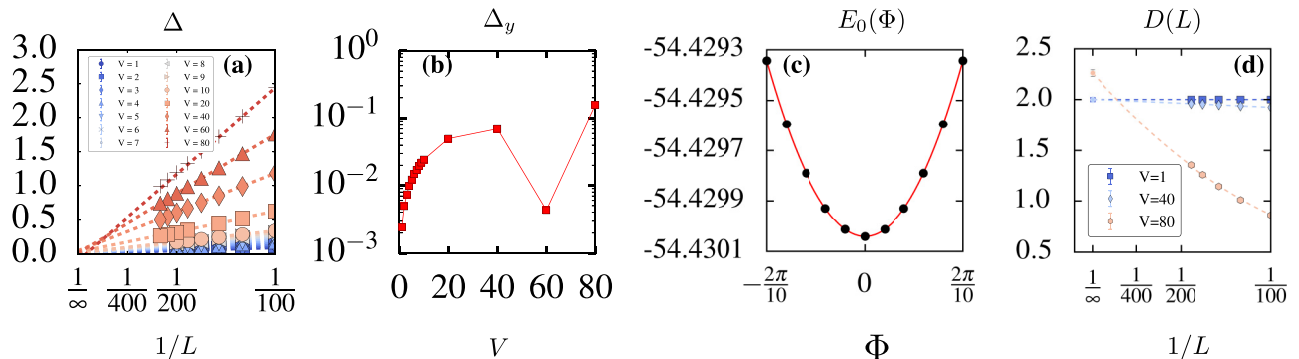

FIG. 8. (a) Finite-size scaling of the single-particle gap Δ for different V. The compressibility $y \equiv \frac{\delta\Delta}{\delta(1/L)}$ is obtained by fitting the numerical data with $\Delta(L) = b + c/L$ (dotted lines). (b) Standard error in the compressibility as a function of V obtained from the least-square (Levenberg-Marquardt) method. (c) Ground state energy $E_0(\Phi)$ as a function of the flux Φ for $V = 1$ and $L = 200$. The red line is the best fit of the form $E_0(\Phi) = a + b\Phi + (c/2)\Phi^2$, where the standard error on E_0 reported in Fig. 7 is included in the final estimate of the fit parameters. The charge stiffness D [$\propto$ the second derivative of $E_0(\Phi)$] is extracted from the previous fit. (d) Finite-size scaling of the charge stiffness D for different V. The errors bars originating from the fit in (c) are smaller than the symbols and thus not visible. The dotted lines are best fits of the form $D(L) = b + c/L + d/L^2$. The final standard errors are estimated from the least-square method. In all plots $\langle n_i \rangle = 0.5$ (half-filling) and $\alpha = 0.5$.
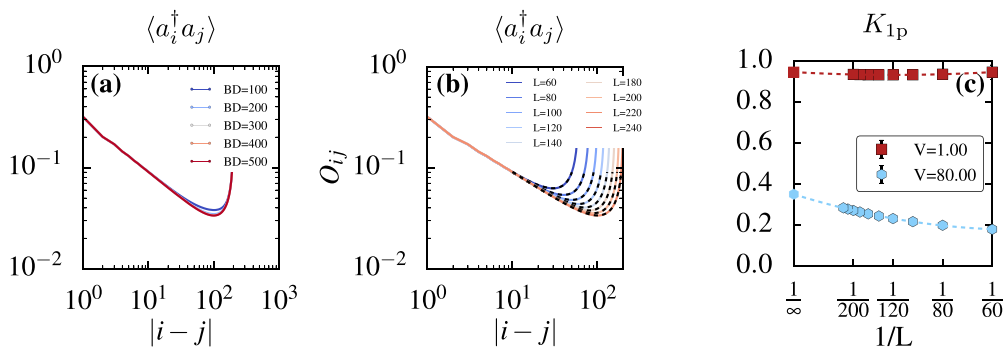
FIG. 9. (a) Single-particle correlation function for different BD for $V = 1$ and $L = 200$. Note that the correlation function on (a) is symmetric with respect to $L/2$. (b) Collapse of the single-particle correlations for different system sizes. We use the fit function (black dotted lines) described in Ref. [76] for a circular chain. The standard error on $K_{1p}(L)$ is obtained from the least-square method. (c) Finite-size scaling of $K_{1p}(L)$ for $V = 1, 80$. The final standard error is again obtained from the least-square method with a fit of the form $K_{1p}(L) = b + c/L + d/L^2$ (red dotted lines). In all plots $\langle n_i \rangle = 0.5$ and $\alpha = 0.5$.

again obtained from the least-square method. In total, the uncertainty Δ_D in the charge stiffness for $L \to \infty$ is $\sim 10^{-3}$.

The Luttinger parameter extracted from the compressibility and the charge stiffness is obtained from the formula $K_{\Delta/D} = \sqrt{D/y}$ (see Sec. IV), and the associated uncertainty reads

$$\Delta_{K_{\Delta/D}} = \frac{1}{2}\sqrt{\frac{D\Delta_y^2}{y^3} + \frac{\Delta_D^2}{yD}}.$$

The latter is shown in Fig. 10(a) as a function of V, and remains $< 10^{-3}$ for all interaction strengths considered in this work.

We now estimate the uncertainties in the single-particle correlation function and the Luttinger parameter K_{1p} plotted in Fig. 5. The convergence of the correlation function with the BD is displayed in Fig. 9(a). In order to extract the upper limit error on the correlation we compute

$$|\langle a_1^\dagger a_{L/2}\rangle(\mathrm{BD} = \infty) - \langle a_1^\dagger a_{L/2}\rangle(\mathrm{BD} = 512)| \approx 10^{-4},$$

where the first term $|\langle a_1^\dagger a_{L/2}\rangle(\mathrm{BD} \to \infty)$ is obtained by extrapolating the ground state energy in the limit of infinite bond dimension.

Fits of the correlation functions for different system sizes (black dotted lines) are shown in Fig. 9(b) using the function

introduced in Ref. [76] for a circular chain (error bars $\sim 10^{-4}$ are not visible). The Luttinger parameter K_{1p} is then extracted from this fit with an error obtained from the least-square method. The extrapolation of K_{1p} in the thermodynamic limit is obtained using a fit of the form $K_{1p}(L) = b + \frac{c}{L} + \frac{d}{L^2}$ and shown in Fig. 9(c). The uncertainty $\Delta_{K_{1p}}$ in the Luttinger parameter K_{1p} in the thermodynamic limit is shown in Fig. 10(b) as a function of V and remains $\sim 10^{-3}$ for all V considered in this work. The standard error on the Luttinger parameter K_{2p} extracted from the two-particle correlations can be obtained with a similar approach and we find that the uncertainty $\Delta_{K_{2p}}$ also remains $\sim 10^{-3}$.

APPENDIX C: EFFECT OF ENERGY EXTENSIVITY ON PLASMON MODES

In this Appendix we consider a one-dimensional system of length L containing N *fermions* interacting via the LR continuous potential

$$V^\alpha(x) = \frac{V}{(x^2 + a^2)^{\alpha/2}}, \quad 0 < \alpha \leqslant 1.$$

Here a denotes a short-distance cutoff that can be identified with, e.g., the lattice spacing. For the sake of convenience we here use fermions instead of hard-core bosons. Indeed the hard-core boson Hamitonian Eq. (1) can be mapped onto an XXZ Heisenberg model (for spins) with long-range z-z coupling, which can itself be mapped onto a fermionic Hamiltonian using the Jordan-Wigner transformation. The two models are thus equivalent, the only difference being the single-particle correlation function

$$\langle c_i^\dagger c_j \rangle \sim r_{i-j}^{-[K+(1/K)]/2}$$

for fermions, while

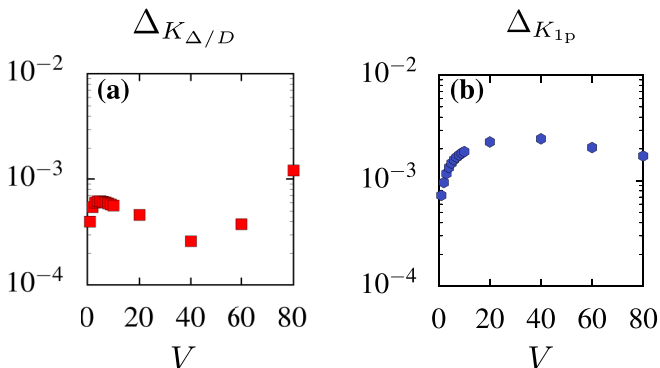$$\langle a_i^\dagger a_j \rangle \sim r_{i-j}^{-1/(2K)}$$

FIG. 10. Final standard errors $\Delta_{K_{\Delta/D}}$ (a) and $\Delta_{K_{1p}}$ (b) in the Luttinger parameter extracted from the compressibility and the charge stiffness, and from the single-particle correlations, respectively, as a function of V.

for hard-core bosons [76]. In the following we use c operators for fermions and a operators for hard-core bosons. In the framework of the 1D Luttinger liquid theory the low-energy Hamiltonian in the vicinity of the Fermi level can be decomposed into the contributions of left (L) and right (R)

movers as

$$H = \sum_k \sum_{r=L,R} \hbar v_F (\eta_r k - k_F) c_{r,k}^\dagger c_{r,k}$$
$$+ \frac{1}{2} \int dx dx' \rho(x) V^\alpha(x - x') \rho(x'), \qquad (C1)$$

where v_F is the Fermi velocity, k_F is the Fermi wave vector, $\eta_R = +1$, $\eta_L = -1$, and $\rho(x) = \sum_{r=L,R} \rho_r(x)$ with $\rho_r(x) = \frac{1}{L} \sum_{k,q} e^{iqx} c_{r,k+q}^\dagger c_{r,k}$. Bosonization assumes that the low-energy properties of the Hamiltonian Eq. (C1) are governed by the long-wavelength fluctuations of the density $\rho(x)$. Using the standard techniques described in Ref. [5], H can be approximately written (for $L \to \infty$) in the quadratic form

$$H = \frac{1}{2\pi} \sum_q \left(u(q) K(q) \pi^2 \Pi(q) \Pi(-q) \right.$$
$$\left. + \frac{u(q)}{K(q)} q^2 \phi(q) \phi(-q) \right),$$

where $u(q)$ denotes the velocity of the excitations and $K(q)$ is the Luttinger parameter governing the decay of correlations at long distances. The latter satisfy the relations

$$u(q) K(q) = v_F, \qquad \frac{u(q)}{K(q)} = v_F \left[1 + \frac{V^{(\alpha)}(q)}{\pi v_F} \right]. \qquad (C2)$$

The Fourier transform of the interaction potential reads

$$V^\alpha(q) = \int dx \, V^\alpha(x) e^{-iqx}$$
$$= V \frac{2\sqrt{\pi}}{\Gamma(\frac{\alpha}{2}) 2^{\frac{\alpha-1}{2}}} \left(\frac{|q|}{a} \right)^{\frac{\alpha-1}{2}} \mathcal{K}_{\frac{\alpha-1}{2}}(a|q|), \qquad (C3)$$

with $\mathcal{K}_\nu$ the modified Bessel function of order ν and Γ the gamma function. The two fields $\Pi(q) = \int dx \, \Pi(x) e^{-iqx}$ and $\phi(q) = \int dx \, \phi(x) e^{-iqx}$ are the Fourier transforms of the canonically conjugate fields $\Pi(x) = \frac{1}{\pi} \nabla \theta(x)$ and $\phi(x)$, with

$$\phi(x) = -(N_R + N_L) \frac{\pi x}{L}$$
$$- \frac{i\pi}{L} \sum_{q \neq 0} \frac{1}{q} e^{-\beta|q|/2 - iqx} [\rho_R(q) + \rho_L(q)],$$

$$\theta(x) = (N_R - N_L) \frac{\pi x}{L}$$
$$+ \frac{i\pi}{L} \sum_{q \neq 0} \frac{1}{q} e^{-\beta|q|/2 - iqx} [\rho_R(q) - \rho_L(q)].$$

Here β is a (small) cutoff regularizing the theory, $N_r = \sum_k c_{r,k}^\dagger c_{r,k} - \langle c_{r,k}^\dagger c_{r,k} \rangle$, and $\rho_r(q) = \sum_k c_{r,k+q}^\dagger c_{r,k}$. The plasmon dispersion relation follows from Eq. (C2) and reads

$$\omega(q) = u(q)|q| = v_F |q| \sqrt{1 + \frac{V^{(\alpha)}(q)}{\pi v_F}}. \qquad (C4)$$

The potential Eq. (C3) exhibits a long-wavelength divergence ($q \to 0$), namely $V^\alpha(q) \sim |q|^{\alpha-1}$ for $0 < \alpha < 1$ and $V^\alpha(q) \sim \log|q|$ for $\alpha = 1$. In the latter case, Eq. (C4) provides the 1D plasmon dispersion $\omega(q) \sim |q| \sqrt{\log|q|}$ stemming from Coulomb interactions [38]. When rescaling the interaction
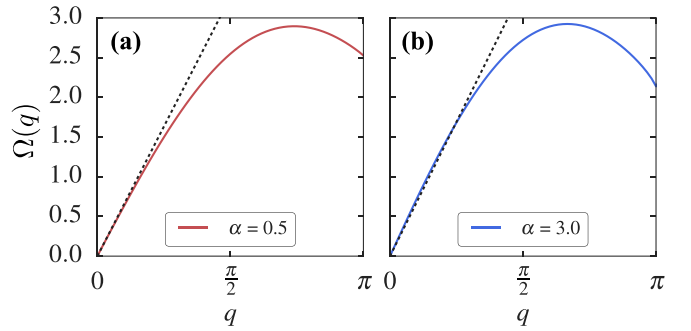

FIG. 11. Upper bound of the excitation spectrum $\Omega(q)$ (in units of t) in the Feynman approximation (colored lines) computed at half-filling for $V = 0.5$ in the strong LR regime $\alpha = 0.5$ (a), and in the short-range case $\alpha = 3$ (b). The dispersion relation Eq. (C4) after Kac's rescaling, namely $\omega(q) = v_F q \sqrt{1 + V/\pi}$ for $\alpha = 0.5$ and $\omega(q) = v_F q \sqrt{1 + V/[\sqrt{\pi} \Gamma(3/2) v_F]}$ for $\alpha = 3$ is represented as a black dotted line in the long-wavelength regime $q \to 0$. The proximity of the Mott transition ($V = 2$ for $\alpha \to \infty$) in the short-range case is responsible for the more pronounced minimum at $q = \pi$ (charge density wave).

potential by the Kac's factor $\Lambda_\alpha(L) = L^{1-\alpha}$ for $0 \leqslant \alpha < 1$ and $\Lambda_\alpha(L) = \log(L)$ for $\alpha = 1$, it is easy to check that the long-wavelength divergence of the potential is removed by considering the limit $q = \frac{2\pi}{L} \to 0$. As a consequence, one recovers the sound wave dispersion relation $\omega(q) \sim |q|$ of a metal with short-range interactions. This result is confirmed by looking at the upper bound of the excitation spectrum $\Omega(q) = E(q)/S(q)$ in the Feynman approximation [77] represented in Fig. 11, where

$$E(q) = \frac{t}{L} [1 - \cos(q)] \left\langle \sum_i a_i^\dagger a_{i+1} + \text{H.c.} \right\rangle$$

and $S(q)$ is the structure factor defined in Eq. (6).

This result can be easily generalized to higher dimensions $d = 2, 3$ by looking at the zeros of the dielectric function in the framework of the random phase approximation (RPA):

$$\epsilon(\mathbf{q}, \omega) = 1 - \chi(\mathbf{q}, \omega) V^\alpha(\mathbf{q}) = 0, \qquad (C5)$$

where

$$\chi(\mathbf{q}, \omega) = \frac{1}{\mathcal{V}} \sum_\mathbf{k} \frac{n_\mathbf{k} - n_{\mathbf{k}+\mathbf{q}}}{\hbar\omega + E_\mathbf{k} - E_{\mathbf{k}+\mathbf{q}} + i\eta}$$

denotes the one-spin density-density response function (Lindhard function), $\mathcal{V}$ is the volume, and $n_\mathbf{k}$ is the occupation number of a state with wave vector $\mathbf{k}$ and energy $E_\mathbf{k} = \frac{\hbar^2 |\mathbf{k}|^2}{2m}$ (m is the particle mass). For $\alpha = 1$ the Fourier transform of the Coulomb potential is

$$V^1(q) \sim \log|q|, \quad d = 1,$$
$$V^1(\mathbf{q}) \sim \frac{1}{|\mathbf{q}|}, \qquad d = 2,$$
$$V^1(\mathbf{q}) \sim \frac{1}{|\mathbf{q}|^2}, \qquad d = 3. \qquad (C6)$$

In the dynamical limit $\omega \gg |\mathbf{q}| v_F$ the Lindhard function can be approximated by $\chi(\mathbf{q}, \omega) = \frac{\rho_0 |\mathbf{q}|^2}{m\omega^2}$, with ρ_0 the average

fermion density. Using this expression together with Eq. (C6) into Eq. (C5), one finds the plasmon energies

$$\omega \sim |q|\sqrt{\log|q|}, \quad d = 1,$$
$$\omega \sim \sqrt{|\mathbf{q}|}, \quad\quad d = 2,$$
$$\omega \sim \text{cst}, \quad\quad\quad d = 3. \quad\quad (C7)$$

When using the Kac's prescription, namely dividing the potential by the factor L^{d-1}, the long-wavelength divergence $(q = \frac{2\pi}{L} \to 0)$ is removed and one recovers the sound wave dispersion relation $\omega \sim |\mathbf{q}|$ for $d = 1, 2, 3$, as for a liquid with purely short-range interactions (e.g., normal He-3).

APPENDIX D: THE INFINITE-RANGE CASE

In the infinite-range case $\alpha = 0$ the Hamiltonian Eq. (1) takes the form of a mean-field Hamiltonian

$$H = -t \sum_{i=0}^{L-1}(c_i^\dagger c_{i+1} + \text{H.c.}) + \frac{V}{2L} \sum_{i \neq j} n_i n_j, \quad (D1)$$

where c_i ($c_i^\dagger$) annihilates (creates) a fermion on site $i = 1, \ldots, L$, and $n_i = c_i^\dagger c_i$ is the local density. Note that we here again use fermions instead of hard-core bosons for convenience, since the two models are equivalent. Considering $N \equiv \sum_i \langle n_i \rangle = L/2$ (with, e.g., N even) fermions in the ground state (half-filling) with antiperiodic boundary conditions, the energy of the ground state is

$$E_0(N) = \frac{N(N-1)V}{2L} - 2t \sum_{k=-L/4}^{L/4-1} \cos\left[\frac{2\pi k}{L} + \left(\frac{\pi}{L}\right)\right]$$
$$= \frac{N(N-1)V}{2L} - 2t \csc\left(\frac{\pi}{L}\right).$$

One then has to consider periodic boundary conditions for $N \pm 1$ fermions, which leads to

$$E_0(N+1) = \frac{(N+1)NV}{2L} - 2t \sum_{k=-L/4}^{L/4} \cos\left(\frac{2\pi k}{L}\right)$$
$$= \frac{(N+1)NV}{2L} - 2t \cot\left(\frac{\pi}{L}\right),$$

$$E_0(N-1) = \frac{(N-1)(N-2)V}{2L} - 2t \sum_{k=-L/4+1}^{L/4-1} \cos\left(\frac{2\pi k}{L}\right)$$
$$= \frac{(N-1)(N-2)V}{2L} - 2t \cot\left(\frac{\pi}{L}\right).$$

The charge gap thus reads $\Delta \equiv E_0(N+1) + E_0(N-1) - 2E_0(N) = (V/L) + 4t \tan(\frac{\pi}{2L})$. For $L \to \infty$ one has $\Delta \sim (V + 2\pi t)/L \to 0$. The Luttinger parameters u/K and uK can be related to the first derivative of the single-particle charge gap as $\frac{\partial \Delta}{\partial (1/L)} = \pi \frac{u}{K}$, and to the charge stiffness [5] as

$$D = \pi L \left| \frac{\partial^2 E_0(N, \Phi)}{\partial \Phi^2} \right|_{\Phi=0} = uK.$$

Here $\Phi = 2\pi \phi / \phi_0$ denotes a flux threading the (circular) chain in units of the flux quantum $\phi_0 = h/e$. This flux can

be taken into account by multiplying the hopping energy by an Aharonov-Bohm phase phase $e^{\pm i\Phi/L}$, which leads to

$$H(\Phi) = -t \sum_{i=0}^{L-1}(e^{i\Phi/L} c_i^\dagger c_{i+1} + \text{H.c.}) + \frac{V}{2L} \sum_{i \neq j} n_i n_j.$$

The energy of the ground state is then derived as

$$E_0(N, \Phi) = \frac{N(N-1)V}{2L} - 2t \csc\left(\frac{\pi}{L}\right) \cos\left(\frac{\Phi}{L}\right),$$

which provides $D = 2t = v_F$ for $L \to \infty$. The Luttinger parameters extracted from the charge gap and from the charge stiffness thus read

$$uK = v_F, \quad \frac{u}{K} = v_F\left[1 + \frac{V}{\pi v_F}\right], \quad (D2)$$

and coincide exactly with the analytic prediction Eq. (3). On the other hand, it is straightforward to calculate the Luttinger parameter K from the single-particle correlation function

$$\langle c_i^\dagger c_j \rangle = \frac{1}{L} \sum_k e^{ik(i-j)} n_k = \frac{1}{2i\pi} \frac{e^{ik_F(i-j)}}{i-j} \sim (i-j)^{-1}, \quad (D3)$$

and from the long-wavelength limit of the static structure factor

$$S(q) \equiv \frac{1}{L} \sum_{i,j} e^{iq(i-j)}(\langle n_i n_j \rangle - \langle n_i \rangle \langle n_j \rangle)$$
$$= \frac{1}{L} \sum_{k,k'}(\langle c_k^\dagger c_{k-q} c_{k'}^\dagger c_{k'+q} \rangle - \langle c_k^\dagger c_{k-q} \rangle \langle c_{k'}^\dagger c_{k'+q} \rangle)$$
$$\to_{q \to 0} \frac{1}{L}. \quad (D4)$$

Comparing Eqs. (D3) and (D4) to the predictions $\langle c_i^\dagger c_j \rangle \sim (i-j)^{-\frac{K+(1/K)}{2}}$ (for fermions) and $K = LS(q \to 0)$ of the Luttinger liquid theory, we thus find $K = 1$ for all V in disagreement with the result

$$K = \frac{1}{\sqrt{1 + V/(\pi v_F)}}$$

obtained from Eq. (D2). This breakdown of the Luttinger liquid theory for $\alpha = 0$ originates from the fact that the mean-field Hamiltonian Eq. (D1) corresponds to free fermions only in a given charge sector due to the presence of the term $\propto N^2$. While the correlation functions do not involve different charge sectors and therefore simply provide the free fermion result $K = 1$, the charge gap is constructed from the ground state energy in different charge sectors (N and $N \pm 1$), which leads to an additional term $\propto V$ in Eq. (D2).

Alternatively one may also directly compare the spectrum of the Hamiltonian Eq. (D1) to that predicted by the LL theory. Considering a chemical potential $\mu = -\frac{V}{2} + \frac{V}{2L}$ in order to cancel the linear term $\propto N$, the Hamiltonian Eq. (D1) becomes

$$H = -t \sum_{i=1}^{L}(c_i^\dagger c_{i+1} + \text{H.c.}) + \mu \sum_i n_i + \frac{V}{2L} \sum_{i \neq j} n_i n_j$$
$$= -t \sum_{i=1}^{L}(c_i^\dagger c_{i+1} + \text{H.c.}) + \frac{V}{2L}\Delta N^2 + \text{cte}. \quad (D5)$$

where $\Delta N = \sum_{i=1}^{L}(n_i - \langle n_i \rangle)$ is the excess particle number with respect to the ground state (half-filling). Linearizing the dispersion relation of the Hamiltonian Eq. (D5) (in Fourier space) around $k \simeq \pm\frac{\pi}{2}$, we find that the energy $\Delta E \equiv E(\Delta N, M, n) - E_0(N)$ of an excitation with excess particle number ΔN, umklapp number M, and momentum $q = \frac{2\pi n}{L}$ is

$$\Delta E = \frac{2\pi v_{\mathrm{F}}}{L}\left[\left(1 + \frac{V}{\pi v_{\mathrm{F}}}\right)\frac{\Delta N^2}{4} + M^2 + n\right]. \quad (D6)$$

Remarkably, because of the interaction term $\propto V$, the low-energy spectrum of H cannot be matched with that of a Luttinger liquid. Indeed in a Luttinger liquid the excitation spectrum is entirely fixed in terms of the Luttinger parameter K and the velocity v_{F} as [78]

$$\Delta E = \frac{2\pi v_{\mathrm{F}}}{L}\left(\frac{\Delta N^2}{4K} + KM^2 + n\right). \quad (D7)$$

Instead, our model behaves as if it was not described by a single parameter K, but by two independent parameters $K_1 = [1 + V/(\pi v_{\mathrm{F}})]^{-1}$ and $K_2 = 1$ for charge and umklapp excitations, respectively. This is impossible in standard Luttinger liquid theory, where a central result is that the two parameters must be the same.

[1] T. Padmanabhan, Phys. Rep. **188**, 285 (1990).

[2] L. D. Landau and E. M. Lifshitz, *Electrodynamics of Continuous Media*, 1st ed., Course of Theoretical Physics (Pergamon, Oxford, 1960).

[3] D. R. Nicholson, *Introduction to Plasma Theory*, 1st ed., Wiley Series in Plasma Physics (Wiley, New York, 1983).

[4] H. Ritsch, P. Domokos, F. Brennecke, and T. Esslinger, Rev. Mod. Phys. **85**, 553 (2013).

[5] T. Giamarchi, *Quantum Physics in One Dimension* (Clarendon, Oxford, 2003).

[6] J. Stuhler, A. Griesmaier, T. Koch, M. Fattori, T. Pfau, S. Giovanazzi, P. Pedri, and L. Santos, Phys. Rev. Lett. **95**, 150406 (2005).

[7] K.-K. Ni, S. Ospelkaus, M. H. G. de Miranda, A. Pe'er, B. Neyenhuis, J. J. Zirbel, S. Kotochigova, P. S. Julienne, D. S. Jin, and J. Ye, Science **322**, 231 (2008).

[8] L. D. Carr, D. DeMille, R. V. Krems, and J. Ye, New J. Phys. **11**, 055049 (2009).

[9] T. Lahaye, C. Menotti, L. Santos, M. Lewenstein, and T. Pfau, Rep. Prog. Phys. **72**, 126401 (2009).

[10] C. Schneider, D. Porras, and T. Schaetz, Rep. Prog. Phys. **75**, 024401 (2012).

[11] J. W. Britton, B. C. Sawyer, A. C. Keith, C. C. J. Wang, J. K. Freericks, H. Uys, M. J. Biercuk, and J. J. Bollinger, Nature (London) **484**, 489 (2012).

[12] D. S. Jin and J. Ye, Chem. Rev. **112**, 4801 (2012).

[13] A. Bermudez, T. Schaetz, and M. B. Plenio, Phys. Rev. Lett. **110**, 110502 (2013).

[14] P. Richerme, Z.-X. Gong, A. Lee, C. Senko, J. Smith, M. Foss-Feig, S. Michalakis, A. V. Gorshkov, and C. Monroe, Nature (London) **511**, 198 (2014).

[15] P. Jurcevic, B. P. Lanyon, P. Hauke, C. Hempel, P. Zoller, R. Blatt, and C. F. Roos, Nature (London) **511**, 202 (2014).

[16] J. S. Douglas, H. Habibian, C. L. Hung, A. V. Gorshkov, H. J. Kimble, and D. E. Chang, Nat. Photonics **9**, 326 (2015).

[17] S. Baier, M. J. Mark, D. Petter, K. Aikawa, L. Chomaz, Z. Cai, M. Baranov, P. Zoller, and F. Ferlaino, Science **352**, 201 (2016).

[18] M. Schmitt, M. Wenzel, F. Böttcher, I. Ferrier-Barbut, and T. Pfau, Nature (London) **539**, 259 (2016).

[19] L. Chomaz, R. M. W. van Bijnen, D. Petter, G. Faraoni, S. Baier, J. H. Becher, M. J. Mark, F. Wächtler, L. Santos, and F. Ferlaino, Nat. Phys. **14**, 442 (2018).

[20] V. D. Vaidya, Y. Guo, R. M. Kroeze, K. E. Ballantine, A. J. Kollár, J. Keeling, and B. L. Lev, Phys. Rev. X **8**, 011002 (2018).

[21] S. Lepoutre, L. Gabardos, K. Kechadi, P. Pedri, O. Gorceix, E. Maréchal, L. Vernac, and B. Laburthe-Tolra, Phys. Rev. Lett. **121**, 013201 (2018).

[22] Y. Tang, W. Kao, K.-Y. Li, and B. L. Lev, Phys. Rev. Lett. **120**, 230401 (2018).

[23] N. Defenu, A. Trombettoni, and S. Ruffo, Phys. Rev. B **94**, 224411 (2016).

[24] N. Defenu, A. Trombettoni, and S. Ruffo, Phys. Rev. B **96**, 104432 (2017).

[25] N. Defenu, T. Enss, M. Kastner, and G. Morigi, Phys. Rev. Lett. **121**, 240403 (2018).

[26] A. Dutta and J. K. Bhattacharjee, Phys. Rev. B **64**, 184106 (2001).

[27] N. Laflorencie, I. Affleck, and M. Berciu, J. Stat. Mech.: Theory Exp. (2005) P12001.

[28] D. Peter, S. Müller, S. Wessel, and H. P. Büchler, Phys. Rev. Lett. **109**, 025303 (2012).

[29] P. Hauke, F. M. Cucchietti, M. Müller-Hermes, A. Bañuls, J. I. Cirac, and M. Lewenstein, New J. Phys. **12**, 113037 (2010).

[30] I. Frérot, P. Naldesi, and T. Roscilde, Phys. Rev. B **95**, 245111 (2017).

[31] T. Botzung, D. Vodola, P. Naldesi, M. Müller, E. Ercolessi, and G. Pupillo, Phys. Rev. B **100**, 155136 (2019).

[32] F. J. Burnell, M. M. Parish, N. R. Cooper, and S. L. Sondhi, Phys. Rev. B **80**, 174519 (2009).

[33] L. Pollet, J. D. Picon, H. P. Büchler, and M. Troyer, Phys. Rev. Lett. **104**, 125302 (2010).

[34] B. Capogrosso-Sansone, C. Trefzger, M. Lewenstein, P. Zoller, and G. Pupillo, Phys. Rev. Lett. **104**, 125301 (2010).

[35] D. Vodola, L. Lepori, E. Ercolessi, A. V. Gorshkov, and G. Pupillo, Phys. Rev. Lett. **113**, 156402 (2014).

[36] M. F. Maghrebi, Z.-X. Gong, and A. V. Gorshkov, Phys. Rev. Lett. **119**, 023001 (2017).

[37] G. Masella, A. Angelone, F. Mezzacapo, G. Pupillo, and N. V. Prokof'ev, Phys. Rev. Lett. **123**, 045301 (2019).

[38] H. J. Schulz, Phys. Rev. Lett. **71**, 1864 (1993).

[39] D. W. Wang, A. J. Millis, and S. Das Sarma, Phys. Rev. B **64**, 193307 (2001).

[40] G. Fano, F. Ortolani, A. Parola, and L. Ziosi, Phys. Rev. B **60**, 15654 (1999).

[41] M. Casula, S. Sorella, and G. Senatore, Phys. Rev. B **74**, 245427 (2006).

[42] G. E. Astrakharchik and M. D. Girardeau, Phys. Rev. B **83**, 153303 (2011).

[43] R. M. Lee and N. D. Drummond, Phys. Rev. B **83**, 245114 (2011).

[44] D. Poilblanc, S. Yunoki, S. Maekawa, and E. Dagotto, Phys. Rev. B **56**, R1645(R) (1997).

[45] S. Capponi, D. Poilblanc, and T. Giamarchi, Phys. Rev. B **61**, 13410 (2000).

[46] B. Valenzuela, S. Fratini, and D. Baeriswyl, Phys. Rev. B **68**, 045112 (2003).

[47] Z.-H. Li, J. Phys.: Condens. Matter **31**, 255601 (2019).

[48] D. Ruelle, Helv. Phys. Acta **36**, 183 (1963).

[49] T. Dauxois, S. Ruffo, E. Arimondo, and M. Wilkens, Dynamics and thermodynamics of systems with long-range interactions: An introduction, in *Dynamics and Thermodynamics of Systems with Long-Range Interactions*, edited by T. Dauxois, S. Ruffo, E. Arimondo, and M. Wilkens (Springer, Berlin, 2002), pp. 1–19.

[50] D. Mukamel, in *Dynamics and Thermodynamics of Systems with Long Range Interactions: Theory and Experiments*, edited by A. Campa, A. Giansanti, G. Morigi, and F. Sylos Labini, AIP Conf. Proc. No. 970 (AIP, New York, 2008).

[51] J. Barré, D. Mukamel, and S. Ruffo, Phys. Rev. Lett. **87**, 030601 (2001).

[52] A. Campa, T. Dauxois, and S. Ruffo, Phys. Rep. **480**, 57 (2009).

[53] M. Kastner, Phys. Rev. Lett. **104**, 240403 (2010).

[54] Y. Levin, R. Pakter, F. B. Rizzato, T. N. Teles, and F. P. Benetti, Phys. Rep. **535**, 1 (2014), nonequilibrium statistical mechanics of systems with long-range interactions.

[55] S. Schütz and G. Morigi, Phys. Rev. Lett. **113**, 203002 (2014).

[56] M. Kac, G. E. Uhlenbeck, and P. C. Hemmer, J. Math. Phys. **4**, 216 (1963).

[57] S. A. Cannas and F. A. Tamarit, Phys. Rev. B **54**, R12661(R) (1996).

[58] F. Tamarit and C. Anteneodo, Phys. Rev. Lett. **84**, 208 (2000).

[59] T. Dauxois, V. Latora, A. Rapisarda, S. Ruffo, and A. Torcini, The Hamiltonian mean field model: From dynamics to statistical mechanics and back, in *Dynamics and Thermodynamics of Systems with Long-Range Interactions*, edited by T. Dauxois, S. Ruffo, E. Arimondo, and M. Wilkens (Springer, Berlin, 2002), pp. 458–487.

[60] A. Campa, A. Giansanti, and D. Moroni, J. Phys. A: Math. Gen. **36**, 6897 (2003).

[61] M. Kastner and O. Schnetz, J. Stat. Phys. **122**, 1195 (2006).

[62] C. Anteneodo and C. Tsallis, Phys. Rev. Lett. **80**, 5313 (1998).

[63] C. Anteneodo, Physica A **342**, 112 (2004), proceedings of the VIII Latin American Workshop on Nonlinear Phenomena.

[64] ITensor Library (version 2.0.11), http://itensor.org.

[65] M. Dalmonte, G. Pupillo, and P. Zoller, Phys. Rev. Lett. **105**, 140401 (2010).

[66] P. Schmitteckert and R. Werner, Phys. Rev. B **69**, 195115 (2004).

[67] F. Franchini, *An Introduction to Integrable Techniques for One-Dimensional Quantum Systems*, Lecture Notes in Physics (Springer, New York, 2017).

[68] This phase was referred to as a strange metal in Ref. [47], since a finite gap $\Delta = V$ is found for $L \to \infty$ in the absence of Kac's rescaling. Upon restoring a well-defined thermodynamic limit ($V \to V/L$) we find that the gap $\Delta \sim (V + 2\pi t)/L \to 0$ for $L \to \infty$ consistently with a metallic phase.

[69] W. Kohn, Phys. Rev. **133**, A171 (1964).

[70] We use the fitting function derived in Ref. [76] from conformal field theory with periodic boundary conditions on a ring.

[71] It is worth commenting on an alternative Kac's prescription, which consists of dividing the whole Hamiltonian Eq. (1) by $\Lambda_\alpha(L)$. The behaviors of the correlation function and of the charge stiffness are not affected by such a global rescaling, and are therefore those of an insulator. However, the charge gap vanishes in the thermodynamic limit since the energy of the ground state E_0 is simply replaced by E_0/L, and the system exhibits an hybrid insulating/metallic behavior.

[72] I. S. Tupitsyn and N. V. Prokof'ev, Phys. Rev. Lett. **118**, 026403 (2017).

[73] R. Landig, L. Hruby, N. Dogra, M. Landini, R. Mottl, T. Donner, and T. Esslinger, Nature (London) **532**, 476 (2016).

[74] C. Maschler and H. Ritsch, Phys. Rev. Lett. **95**, 260401 (2005).

[75] M. O. Scully and M. S. Zubairy, *Quantum Optics* (Cambridge University Press, Cambridge, 1997).

[76] M. A. Cazalilla, J. Phys. B: At., Mol. Opt. Phys. **37**, S1 (2004).

[77] G. G. Batrouni, F. F. Assaad, R. T. Scalettar, and P. J. H. Denteneer, Phys. Rev. A **72**, 031601(R) (2005).

[78] V. E. Korepin, N. Bogoliubov, and A. G. Izergin, *Quantum Inverse Scattering Method and Correlation Functions* (Cambridge University Press, Cambridge, 1993).